ISAS - INTERNATIONAL SCHOOL
FOR ADVANCED STUDIES

First-principles study of structural and dynamical properties of II-VI semiconductors and their alloys

Thesis submitted for the degree of
"Magister Philosophiæ"

CANDIDATE
Andrea DAL CORSO

SUPERVISORS
Prof. Stefano BARONI
Prof. Raffaele RESTA

April 1992

TRIESTE

SISSA - SCUOLA
INTERNAZIONALE
SUPERIORE
STUDI AVANZATI
TRIESTE
Strada Costiera 11

SISSA ISAS

SCUOLA INTERNAZIONALE SUPERIORE DI STUDI AVANZATI
INTERNATIONAL SCHOOL FOR ADVANCED STUDIES

First-principles study of structural and dynamical properties of II-VI semiconductors and their alloys

Thesis submitted for the degree of

"Magister Philosophiæ"

CANDIDATE

Andrea DAL CORSO

SUPERVISORS

Prof. Stefano BARONI

Prof. Raffaele RESTA

April 1992

I - Introduction

A ferroelectric phase transition has been recently observed in the ternary alloy $Zn_xCd_{1-x}Te$ [1]: this is the first report of ferroelectricity in a material which has the zincblende structure in its paraelectric phase. The phase transition is clearly indicated by the increase of the dielectric constant near the transition temperature (T_c), and by the observation of the polarization hysteresis loop below T_c. The transition temperature is in the range 100–250 C and the absolute value of the residual polarization is $\simeq 5\ nC/cm^2$, fairly small with respect to typical values found in other ferroelectric materials.

Ferroelectricity has been found in samples with concentration $x = 0.1$, $x = 0.3$, $x = 0.45$; in all cases X-ray diffraction studies [2] have shown a rhombohedral crystal structure, with an angle $\alpha = 89.4°$. The mixed (Cd-Zn) sublattice is basically undistorted, while Te atoms are displaced with respect to the ideal zincblende position, by about $\simeq 0.11$ Å, *independently of* x. Previously to the discovery of ferroelectricity, this same alloy was studied via EXAFS [3] at room temperature, i.e. *below* T_c: such measurements indicated in fact anion displacements of the same order as found from the analysis of later X-ray diffraction data. The distortion of the anion sublattice is in agreement with the general understanding of ternary semiconductor alloys, although in a

disordered (unpolarized) material the displacements detected via EXAFS are assumed to be incoherent. From a theoretical point of view, II-VI materials—either pure or alloyed—have been studied much less than the III-V's, [4][5] and only a few phenomenological models [6], and some all-electron calculations [7] exists. The purpose of this work is to study some physical properties of the II-VI materials—both pure and alloyed—in the framework of first-principles density-functional theory (DFT). The unexpected phenomenon of ferroelectricity calls for a deeper understanding of these materials.

DFT within local density approximation (LDA), has been able to describe with astonishing precision the structural properties of simple semiconductors, their phonon frequencies, dielectric constants, deformation potentials, piezoelectric constants, effective charges, macroscopic stress acting in a crystal and many other properties. Most of the state-of-the-art work for semiconductors is performed using norm-conserving pseudopotentials and linear-response theory (LRT). The extension of these studies to materials containing group II elements (Zn, Cd, Hg) does not present any conceptual difficulty, but practically *ab-initio* pseudopotential calculations have given until now few encouraging results [8] on these compounds, the only exception being a calculation of the structural properties of ZnS [9], and a calculation of the band offset of GaAs/ZnSe (110) interface [10]. The most serious problem is the presence of cation d electrons with energies of order 10 eV below the valence s electrons. All-electron calculations [11] have shown that d electrons give important contribution to bond

formation both in ZnTe and in CdTe and in II-VI semiconductors in general; actually they form a flat band whose energy is higher than the anion s band and for this reason they should be considered as valence electrons. This cannot be done in practice with the usual plane-wave formalism, because the resulting pseudopotential is too hard to allow converged calculations within reasonable basis sets. One partial solution of this problem has been recently proposed [12] to deal with these difficult cases. The idea is to include d electrons in the frozen core and to compute the correct exchange and correlation energy using the *total*—rather than *valence*—charge density: this is achieved by adding the frozen core charge to the self-consistent valence charge. This approach, known as non linear core correction (NLCC), was first used by Louie, Froyen and Cohen [12] for the description of magnetic systems, but the application to Zn and Cd was not thoroughly investigated until now, the only work being, to our knowledge Refs. 9,10 .

We began investigating structural and dynamical properties of pure ZnTe and CdTe as a preliminary step towards the understanding of the alloy (and possibly of its ferroelectric properties). A further line of investigation, not reported in this thesis, concerns the properties of ZnCdTe superlattices. The original work performed in this thesis is reported in the following sections, which are summarized as follows:

In Sec. II we report the generation of new pseudopotentials for zinc and cadmium, to be used in the framework of NLCC. As a benchmark, we have

studied the structural properties of the two pure compounds.

In Sec. III we generalized Linear Response Theory in the framework of NLCC: this includes the effect of the moving core charge. We have then modified the numerical code used to calculate phonon frequencies at a generic $\mathbf{q}$ point [13] and we have calculated from the first principles the phonon spectra of ZnTe and CdTe along several high symmetry directions of the Brillouin zone.

As a preliminary step towards the study of the alloy we report in Sec. IV the calculated relaxations of the atoms in one prototypical supercell geometry. We show that tellurium sublattice is much more distorted than Zn-Cd one and we obtain a relaxed configuration in agreement with X-ray and EXAFS measurements. Some preliminary considerations about spontaneous polarization and ferroelectricity are also reported.

II - Non Linear Core Correction

Within the usual pseudopotential formulation of DFT, the total energy of the solid is expressed as a functional of the valence (pseudo) charge density (ρ_v) only, as:

$$E_{tot} = T[\rho_v] + E_{ei}[\rho_v] + E_H[\rho_v] + E_{xc}[\rho_v] + E_{ii} \tag{1}$$

where

$$E_{ei} = \int_V V_{ps}\rho_v(r)\mathrm{dr} \tag{2}$$

$$E_H = \frac{1}{2}\int_V \frac{\rho_v(r)\rho_v(r')}{|r-r'|}\mathrm{drdr'} \tag{3}$$

$$E_{xc} = \int_V \epsilon_{xc}(\rho_v)\rho_v\mathrm{dr} \tag{4}$$

$T[\rho_v]$ is the kinetic energy of the non interacting system, calculated using Kohn and Sham orbitals, and E_{ii} is the electrostatic energy of bare ions. In this formulation it is implicitly assumed that the total charge density can be split into a core and a valence contribution, and the energy associated with the core charge is subtracted off. The interaction between core and valence orbitals is completely accounted for by the pseudopotential (V_{ps}), which must be able to correctly represent the effect of the orthogonalization of the valence eigenfunctions to the core ones, the effect of the interaction of a valence electron

with the electrostatic potential of the core charge and the effect of exchange and correlation between valence and core eigenfunctions. The possibility of building a pseudopotential that fulfills all these constraints is linked to the validity of two hypothesis:

(i) Frozen core approximation, meaning that the electronic structure of the core does not depend on the different chemical environment;

(ii) Small overlap between core and valence charge, which is a necessary condition to linearize the exchange and correlation energy.

Both hypotheses are not strictly valid for group II elements if we assume that d electrons are included in the fixed core charge. In particular hypothesis (ii) is clearly violated as can be seen in Fig. 1 where we plot the core and valence charges of Zn and Cd. To deal with these elements in the framework of pseudopotential plane waves theory we have to reconsider hypothesis (ii) and its consequences. The idea is to write the exchange and correlation energy in the form [12]:

$$E_{xc} = \int \epsilon_{xc}(\rho_v + \rho_c)(\rho_v + \rho_c)\mathrm{dr}. \tag{5}$$

This means that we do not linearize Eq. (5) as it is implicitly done in usual pseudopotential calculations, where it is assumed that it is possible to write Eq. (5) in the form :

$$E_{xc} = \int \epsilon_{xc}(\rho_c)\rho_c\mathrm{dr} + \int \epsilon_{xc}(\rho_v)\rho_v\mathrm{dr} + \int \epsilon_{xc}(\rho_v)\rho_c\mathrm{dr} + \int \epsilon_{xc}(\rho_c)\rho_v\mathrm{dr}; \tag{6}$$

the last two term are then supposed to be zero and the first one to be a constant (frozen core approximation). Hypothesis (ii) has been used in many pseudopotential calculations made until now and it is a very good approximation for groups IV, V, VI elements, but it is not completely acceptable in group III atoms, and it is basically wrong in group II atoms.

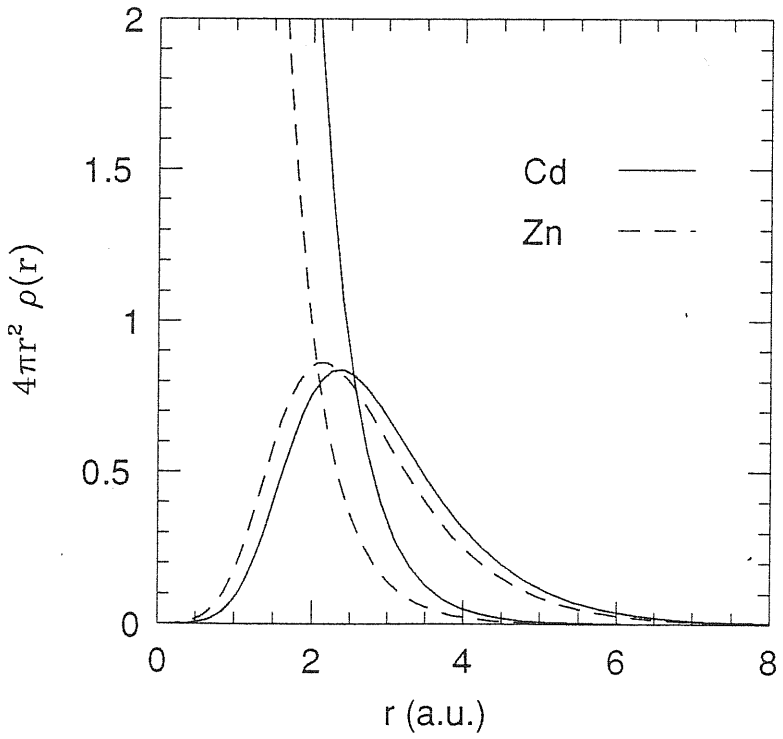

Fig. 1 - Core and valence charge of zinc and cadmium neutral atoms. d electrons are included in the frozen core.

II - a) Generation of the pseudopotentials

In order to calculate exchange and correlation with Eq. (5), the usual ionic pseudopotentials [14] are not correct because they are obtained using Eq. (6). For this reason we had to generate new norm conserving pseudopotentials, and to this end we used the method suggested by von Barth and Car [15]. In this method the form of the pseudopotential is a given function of some parameters, which are determined by minimizing simultaneously the difference among the all-electron atomic eigenvalues and the same eigenvalues calculated for the pseudoatom and the difference between the valence pseudo-eigenfunctions and the all-electron wavefunctions. The latter difference is calculated outside a certain core radius r_c, which is chosen between the last zero and the last maximum of the all-electron eigenfunction. In this formulation the valence charge is exact in the range $r > r_c$, and to correctly reproduce exchange and correlation energy, we have to fit the core charge only in the range $r > r_0$, where $r_0 \simeq r_c$. In the range $0 < r < r_0$ the core charge is smoothed with an arbitrary function chosen is such a way that ρ_c is continuous and derivable:

$$\rho_c = \frac{A \sin Br}{r} \qquad 0 < r < r_0. \tag{7}$$

In order to choose r_0 we have to come to a tradeoff between the accuracy of exchange and correlation and the number of plane waves necessary in the total energy calculation. Tests made in Ref. 12 showed that r_0 can be chosen

in the range where the core charge is from one to two times larger than the valence charge density, and in our case we find no substantial worsening of the results by choosing r_0 as the radius where core and valence charge are equal, using therefore a very smooth core charge. In Fig. 2 and Fig. 3 we display the all-electron valence wavefunctions of Zn^+ and Cd^+ ions together with the pseudowavefunctions.

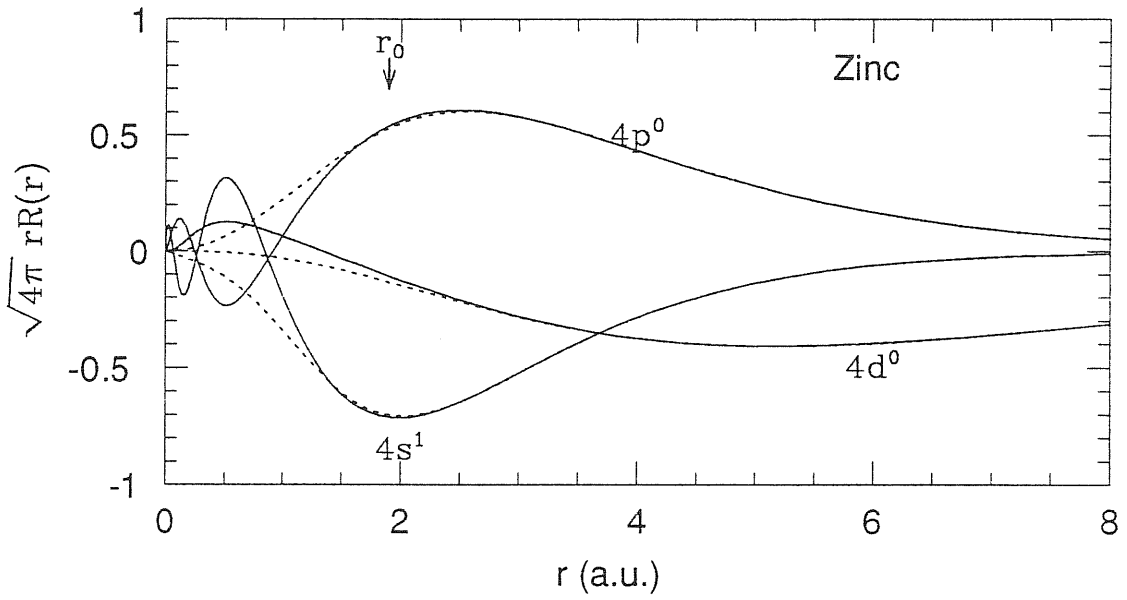

Fig. 2 - All-electron and pseudowavefunctions of Zn ion. r_c is at the maximum of the all-electron eigenfunction, while the vertical line indicates the position of r_0.

The choice of the reference atomic configuration to which pseudowavefunctions are fitted, is a particularly delicate point of the whole procedure. Zinc and cadmium neutral atoms have only s valence electrons but we need to generate

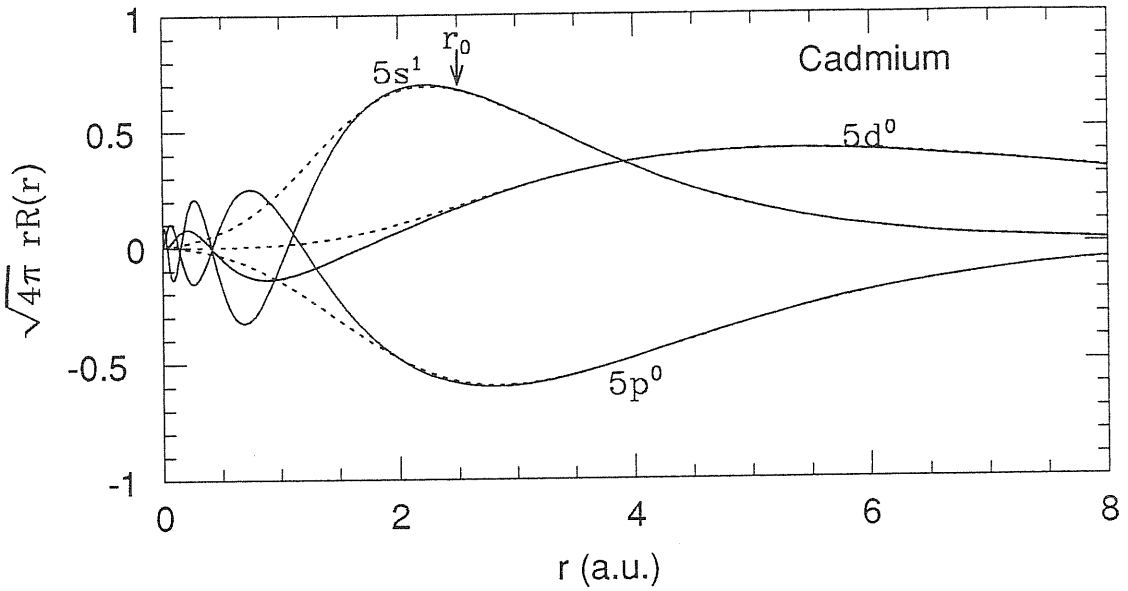

Fig. 3 - All-electron and pseudowavefunctions of Cd ion. r_c is at the maximum of the all-electron eigenfunction, while the vertical line indicates the position of r_0.

the s, p and d components of the non local pseudopotential: this gives us the freedom of choosing the configuration for the p and d components of the pseudopotential. One possibility is to calculate the p and d levels of the most external shell using an excited configuration; but we found that the resulting eigenfunctions are too spread in space to be efficiently fitted, so we choose the lowest s, p and d empty levels of the positive ions Zn^+ and Cd^+. As a test of transferability we then calculated the neutral atom s valence eigenvalue with the result shown in the first line of Table I:

E(R.)	Zn All-el.	Pseudowf.	ΔE	Cd All-el.	Pseudowf.	ΔE
s^2	-0.451	-0.457	0.006	-0.432	-0.437	0.005
s^1	-1.538	-1.538	0.0	-0.9895	-0.9886	0.0009
p^0	-0.5881	-0.5881	0.0	-0.5591	-0.5599	0.0008
d^0	-0.1668	-0.1668	0.0	-0.1694	-0.1698	0.0004

Table I - Energy eigenvalues of the all-electron zinc and cadmium atoms compared with the pseudopotential values. The first row refers to neutral configuration, while the others refer to the ions.

In the remaining lines of the table we report the values of all-electron atomic eigenvalues and those of the pseudoatom for the ionized configuration. All-electron calculations are fully relativistic but spin orbit interaction is not included. We used the exchange and correlation energy calculated by Ceperley and Alder in the parameterization of Perdew and Zunger [16].

II - b) Structural properties of ZnTe and CdTe

We have tested the quality of the pseudopotentials by calculating the lattice constant and bulk modulus of pure ZnTe and CdTe. These compounds crystallize in the zincblende structure. The method used is the standard one that consists in calculating the total energy with a fixed kinetic energy cut-off

for a few lattice parameters and in fitting the energies with some equation of state. We used Murnaghan equation [17]:

$$E = \frac{\Omega_0 B_0}{B_0'}\left[\frac{1}{B_0'-1}\left(\frac{\Omega_0}{\Omega}\right)^{B_0'-1} + \frac{\Omega}{\Omega_0}\right] + cost. \tag{8}$$

This formula has three adjustable parameters: the equilibrium volume of the cell Ω_0, the bulk modulus B_0 and the derivative of the bulk modulus B_0' with respect to the pressure. These are fitted to the calculated values of the energy. The result of the interpolation for various values of the fixed cut-off can be seen in Table II. These values show that a kinetic energy cut-off of 16 Ryd is sufficient to give accurate results of the lattice constant and of bulk modulus for both systems. This cut-off leads to approximately 500 plane waves at the equilibrium volume. For Brillouin zone integration we used the grid (444) by Monkhorst-Pack corresponding to the set of 10 Chadi-Cohen points in the irreducible wedge [18].

(a.u.),(Kbar)	14 Ryd	16 Ryd	20 Ryd	24 Ryd	exp
a_0 (ZnTe)	11.47	11.48	11.47	11.47	11.48
B_0 (ZnTe)	519	516	524	521	506
B_0' (ZnTe)	4.6	4.6	4.5	4.4	—
a_0 (CdTe)	12.21	12.19	12.19	12.19	12.25
B_0 (CdTe)	472	490	475	480	450
B_0' (CdTe)	4.2	4.7	4.5	4.5	4.2

Table II - Lattice constant, bulk modulus and derivative of the bulk modulus with respect to the pressure, calculated for different kinetic energy cut-off.

III - Linear Response Theory within NLCC

A large number of observable ground state properties of a solid can be calculated as derivatives of the total energy with respect to a parameter. For instance, the two quantities we want to discuss—force acting on an atom in a distorted configuration and harmonic force constants—can be obtained as the first and second derivative with respect to the atomic position. The derivative can be evaluated either by finite differences, by subtracting the result of two self consistent calculations for two different configurations of the solid, or analytically, through the Hellmann-Feynman theorem [19]. The finite-differences method is limited by the fact that a large number of perturbations of interest breaks the translation symmetry of the solid: the energy of the perturbed configuration can therefore be obtained only at the price of using large supercells. This is the reason why only phonon frequencies at high-symmetry points of the Brillouin zone have been calculated in this way [20]. This approach is known as the "frozen-phonon" method.

The linear response does not require high-symmetry distortions. The forces acting on an atom can be obtained using only the unperturbed charge density; moreover using the variation of the charge linearly induced by the perturbation it is possible to calculate second derivatives of the energy and, from these,

phonon frequencies. Recently a new method [21] has been introduced to perform a self consistent calculation that gives exactly the linear variation of the charge produced by any perturbation. Implementations of this analytic-derivative scheme have been applied to the calculation of the dielectric constants, effective charges, piezoelectric constants and phonon frequencies [13][22] of the most common semiconductors of group IV and of groups III-V. We want to extend these same techniques to II-IV semiconductors (ZnTe and CdTe) and to this end, the NLCC must be explicitly accounted for in the LRT. The most important point to note is that whenever exchange and correlation involve the core charge, a variation of the position of the atom implies a variation of the exchange and correlation potential. The resulting force has been recently discussed [9][23], but the contribution to the harmonic force has not been reported in the literature [24].

Here we present the necessary generalization of the LRT that is applicable when the perturbation is generated by an atomic displacement: this amounts to displace both the pseudopotential and the core charge. The starting point is Eq. (1), where exchange and correlation are given by Eq. (5). For the sake of clarity, the presentation given here is limited to local pseudopotentials; all of the calculation are performed indeed using non local pseudopotentials, where the corresponding expressions look more complex. We are interested in the second derivative with respect to two general parameters λ and μ. Within lattice dynamics, each of the two parameters is identified with one component

of the displacement $u_s(R)$ of the atom s (whose equilibrium position is τ_s) in a cell characterized by the Bravais vector R. The core charge of the solid is given by:

$$\rho_c(r) = \sum_R \sum_s \rho_c^s(r - R - \tau_s - u_s(R)), \tag{9}$$

and contains explicitly the parameter with respect to which we derive. In this case Hellmann-Feynman theorem becomes:

$$\frac{\partial E_{tot}}{\partial \lambda} = \int_V \rho_v(r) \frac{\partial V_{ps}}{\partial \lambda} \mathrm{d}^3\mathrm{r} + \int_V V_{xc}(\rho_{tot}) \frac{\partial \rho_c}{\partial \lambda} \mathrm{d}^3\mathrm{r} \tag{10}$$

where V_{xc} has the usual definition as the derivative of the exchange and correlation energy with respect to the density. The first term is the well known expression for the force, while the second one is the contribution due to NLCC. The harmonic force can be obtained by deriving with respect to a second parameter μ:

$$\begin{aligned} \frac{\partial E_{tot}}{\partial \mu \partial \lambda} = & \int_V \frac{\partial \rho_v(r)}{\partial \mu} \frac{\partial V_{ps}}{\partial \lambda} \mathrm{d}^3\mathrm{r} + \int_V \rho_v(r) \frac{\partial^2 V_{ps}}{\partial \mu \partial \lambda} \mathrm{d}^3\mathrm{r} \\ & + \int_V \frac{\partial V_{xc}}{\partial \rho_{tot}} \left(\frac{\partial \rho_v}{\partial \mu} + \frac{\partial \rho_c}{\partial \mu} \right) \frac{\partial \rho_c}{\partial \lambda} \mathrm{d}^3\mathrm{r} \\ & + \int_V V_{xc}(r) \frac{\partial^2 \rho_c}{\partial \mu \partial \lambda} \mathrm{d}^3\mathrm{r}. \end{aligned} \tag{11}$$

If we consider the variation of the Kohn e Sham potential [25]:

$$\frac{\partial V_{KS}}{\partial \lambda} = \frac{\partial V_{ps}}{\partial \lambda} + \frac{\partial V_H}{\partial \lambda} + \frac{\partial V_{xc}}{\partial \rho_{tot}} \left(\frac{\partial \rho_c}{\partial \lambda} + \frac{\partial \rho_v}{\partial \lambda} \right) \tag{12}$$

we see that the introduction of NLCC is equivalent, as far as the variation of the valence charge is concerned, to an effective external potential given by:

$$\Delta V_{eff} = \Delta V_{ps} + \frac{\partial V_{xc}}{\partial \rho_{tot}} \Delta \rho_c \tag{13}$$

and the harmonic force constant can be expressed as the usual force constant with the effective variation of the external potential plus two terms that do not depend on the variation of the valence charge:

$$\frac{\partial E_{tot}}{\partial\mu\partial\lambda} = \frac{\partial E^0_{tot}}{\partial\mu\partial\lambda} + \int \frac{\partial V_{xc}}{\partial\rho_{tot}} \frac{\partial\rho_c}{\partial\mu} \frac{\partial\rho_c}{\partial\lambda} \mathrm{d}^3\mathrm{r} + \int V_{xc}(r) \frac{\partial^2\rho_c}{\partial\mu\partial\lambda} \mathrm{d}^3\mathrm{r}. \qquad (14)$$

These results have been implemented in a code for lattice dynamics and applied to the computation of phonon frequencies of ZnTe and CdTe along lines of high symmetry. Plane waves up to 16 Ryd have been used: this is enough to provide a numerical accuracy of the order of 8 cm^{-1} on the calculated phonon frequencies. The other computational details are the same as in Ref. 13. We report in Table III our theoretical values for the Born effective charges and dielectric constants for the two materials; the experimental data are shown as well, after Ref. 26 for CdTe and Ref. 27 for ZnTe

	ZnTe	exp	CdTe	exp
ϵ_∞	8.35	7.28	7.76	7.1
Z^*	2.05	2.0	2.18	2.35

Table III - Born effective charges and dielectric constants of ZnTe and CdTe. The values correspond to a kinetic energy cut-off of 16 Ryd.

The phonon spectra have been measured in the early seventies through neutron scattering (Ref. 28 for ZnTe and Ref. 26 for CdTe), and they were interpolated using shell model with 14 parameters [28] and rigid ion model using

11 parameters [27]. Experimental error on optical branches of CdTe is of the order of 8 cm^{-1}, but infrared measurements at the zone center also exist [29], which are in substantial agreement with neutron data and have smaller errors (a few cm^{-1}).

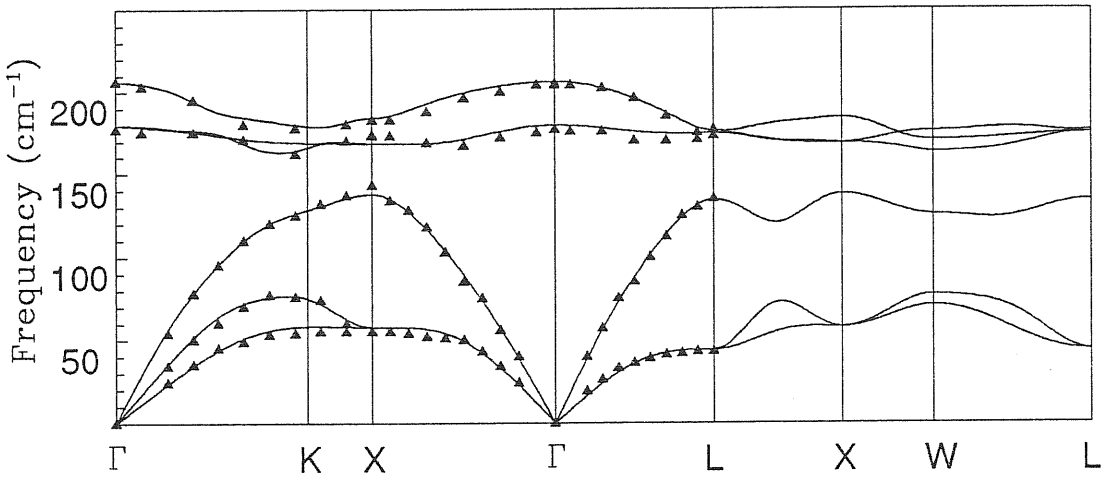

Fig. 4 - Phonon spectra of ZnTe along high-symmetry directions. Experimental points are from reference Ref. 28. Continuous line is the first-principles result.

Our calculated spectra are reported and compared with experimental data in Fig. 4 and Fig. 5. The present results demonstrate the possibility of using NLCC to account quite satisfactorily for the effect of d electrons of group II elements within a pseudopotential formulation. The difference between calculated and measured frequencies is never larger than 10 cm^{-1} and it is

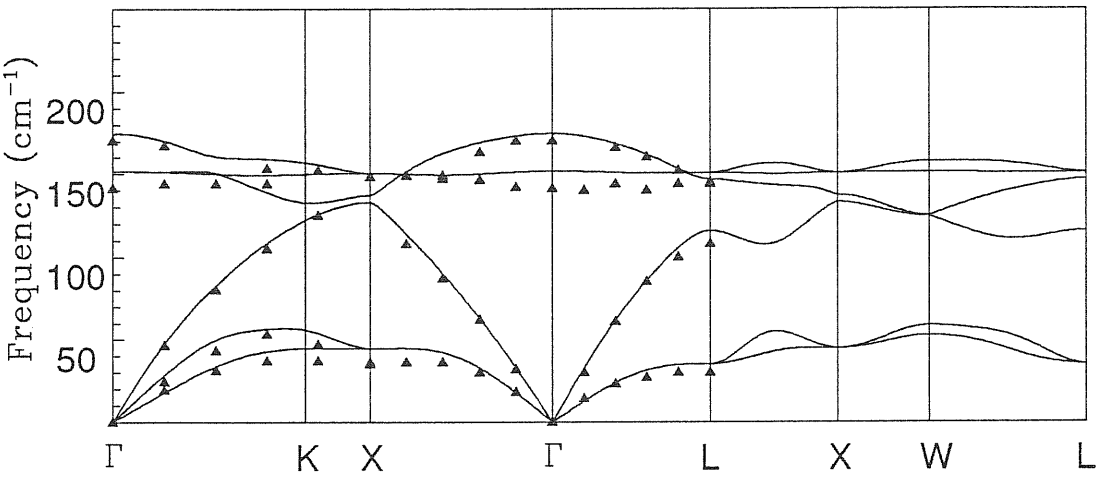

Fig. 5 - Phonon spectra of CdTe along high-symmetry directions. Experimental points are from reference Ref. 26. Continuous line is the first-principles result.

much larger in CdTe than in ZnTe. This error is probably due to relaxation of d electrons not accounted for by our approximation. Our result for lattice dynamics indicates that NLCC correctly reproduces bond bending and bond stretching in the II-VI's, even for low symmetry configurations. This gives confidence in the reliability of the approximations for use in the $Zn_xCd_{1-x}Te$ alloy calculations for structural properties, in particular for cases where low symmetry ionic configurations are involved.

IV - Zn_x Cd_{1-x} Te alloy and ferroelectricity

A ferroelectric crystal is a solid which—below a critical temperature T_c—exhibits a spontaneous polarization; in general the polarization may be reoriented under the influence of an applied electric field. Ferroelectric crystals can be classified into several classes, and different models have been used to explain their behaviour. One class contains systems like KH_2PO_4 where ferroelectricity is associated with the tunneling of hydrogen atoms between different sites and with a transition form a disordered to and ordered configuration. A second class of ferroelectric materials consists of ionic crystals with crystal structures closely related to the perovskite structure. Examples are $BaTiO_3$, $KNbO_3$, $PbTiO_3$. In this class the transition is characterized by a decrease of the frequency of one optical transverse phonon at zone center which vanishes when the transition temperature is reached from above. Below T_c the optical mode is unstable and the crystal distorces towards a polarized structure. Finally there is a third class that contains some narrow-gap semiconductors such as PbTe whose dielectric constant increases by decreasing the temperature but it does not diverge at any finite temperature. Also GeTe belongs to this class. It shows a transition from rocksalt structure at high temperature to a trigonal ferroelectric structure. In this case the high conductivity prevents any direct

measurement of the static dielectric constant.

In the alloy $Zn_xCd_{1-x}Te$ a fraction of zinc atoms substitutes cadmium in the II-VI semiconductor CdTe. None of the two pure compounds is ferroelectric, but the introduction of a small quantity of zinc in CdTe makes the alloy ferroelectric with a critical temperature that depends on composition an varies between $T_c = 90$ C at $x = 0.05$ to $T_c = 250$ C at $x = 0.45$ [1].

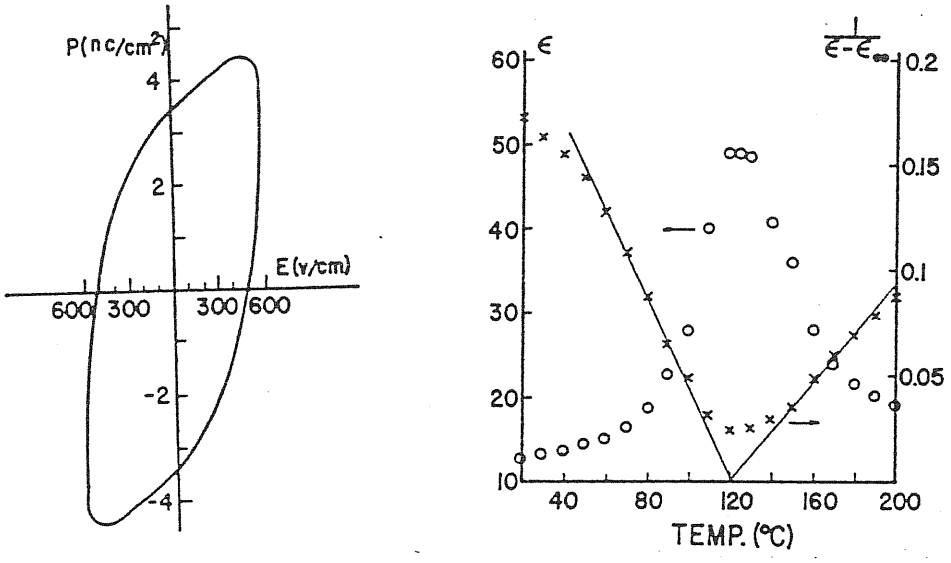

Fig. 6 - Experimental dielectric function, and hysteresis loop of the alloy with x=0.1. Data are from Ref. 1.

Experimental data reported in Fig. 6 are relative to $x = 0.1$. A clear increase of dielectric constant in (111) direction, and the measurement of the hysteresis loop in the dependence of polarization on applied electric field, seem

to suggest the presence of a ferroelectric transition, even if the maximum value of ϵ ($\epsilon_{max} = 50$) and the value of typical polarization ($P = 5\ nC/cm^2$), are much smaller than the values measured in typical ferroelectrics ($\epsilon_{max} = 10^3 - 10^4$, $P = 0.1 - 100\mu C/cm^2$). In this case it is difficult to unambiguously classify the transition according to some known model even if initially the possibility was suggested [1] that ferroelectricity could be associated with an order-disorder phenomenon related to a displacement of zinc atom inside the tetrahedron of tellurium atoms, in analogy with the alloy $Pb_{1-x}Ge_xTe$ [30], where the large difference in atomic radii between Pb and Ge seems to drive the transition.

Semiconductor alloys have been the subject of intensive studies in last few years. Even if there was no indication of the possibility of a ferroelectric phase transition, a great effort has been devoted to the characterization of local properties of these compounds [3], and to the study of possible ordered structures. Different approaches have been applied in the study of alloys of the type $A_xB_{1-x}C$, particularly for III-V semiconductors, the most successful being due to Zunger and coworkers [5]. The results of EXAFS measurements [31] have shown that A and B cations sit on a fcc lattice, which is practically undistorted. The approach of Zunger [5] exploits this feature and starts from the tetrahedra having four cations at the vertices as fundamental units, where the embedded anion is generally off center. There are five possible arrangements: A_4C, A_3BC, A_2B_2C, AB_3C, B_4C. In general, in all these structures, bonds are distorted with respect to the ideal geometry of the binary crystal, but it is

possible to characterize the local properties of the alloy using a single parameter Δ which describes the position of the off center anions along (111). Using DFT within LDA it is possible to calculate the lattice equilibrium constant, the energy, and the parameter Δ for every fundamental tetrahedron and to extract the properties of the alloy from the average. For the particular alloy we are interested in, EXAFS measurement have been reported [3] long before the finding of ferroelectricity. In this case the great difference between bond lengths of the two pure compounds (0.163 Å) makes it possible to distinguish unambiguously two type of cations at slightly different distances from the anions. Defining

$$\epsilon(x) = \frac{d_{ZnTe}(x) - d_{CdTe}(x)}{r_{ZnTe} - r_{CdTe}} \tag{15}$$

where d are the distances in the alloy and r in the pure compounds, the value $\epsilon = 0.75$ is obtained practically independently of alloy composition.

Following the measurement of ferroelectricity also diffraction by X-ray experiments have been reported [2] and the results have been interpreted supposing that Zn-Cd lattice is distorted to a rhombohedral structure with an angle $\alpha = 89.4°$ (very close to the undistorted structure where $\alpha = 90°$), and the lattice constant depend on composition according to the Vegard law:

$$a_{alloy} = a_{ZnTe}x + a_{CdTe}(1 - x). \tag{16}$$

Most important, the tellurium sublattice is distorted below T_c, and every tellurium atom is in a position that depends on the kind of its neighbours,

and that makes Zn-Te and Cd-Te bonds almost of the same length of the pure compounds. The X-ray data have been interpolated supposing that, below T_c tellurium atoms are displaced in (111) direction of an amount $\Delta = 0.1 \pm 0.02$ Å with respect to the ideal zincblende position.

While an all-electron calculation [32] of electronic and structural properties of the alloy $Zn_xCd_{1-x}Te$ exists, no *ab-initio* pseudopotential study has been reported so far on this system. A naif hypothesis about the nature of ferroelectricity relies on displacements of Zn atoms, due to its small atomic radius with respect to the average atomic cell size. This hypothesis is not supported by EXAFS and X-ray data, which show the cationic sublattice as almost undistorted. Nonetheless we have checked this hypothesis in a straightforward way, studying the stability of ZnTe at an expanded lattice constant. Choosing the lattice constant of CdTe, the energy as a function of zinc position along (111) is shown in Fig. 7. As it is easily seen, there is no tendency to softening anyhow, the zincblend position being the most stable. Such a simple mechanism cannot therefore be invoked to explain an order-disorder transition.

Possible relaxation seems to be connected with the properties of the mixed system. The alloy model we decided to study is the simplest system which has the same local properties of the alloy at $x = 0.5$: a superlattice along (111) with four atoms per cell. Considering the trigonal cell shown in Fig. 8 and repeating it in a Bravais lattice we obtained a superlattice composed by alternating planes Zn-Te-Cd-Te-Zn..., in which the two tellurium atoms are not equivalent.

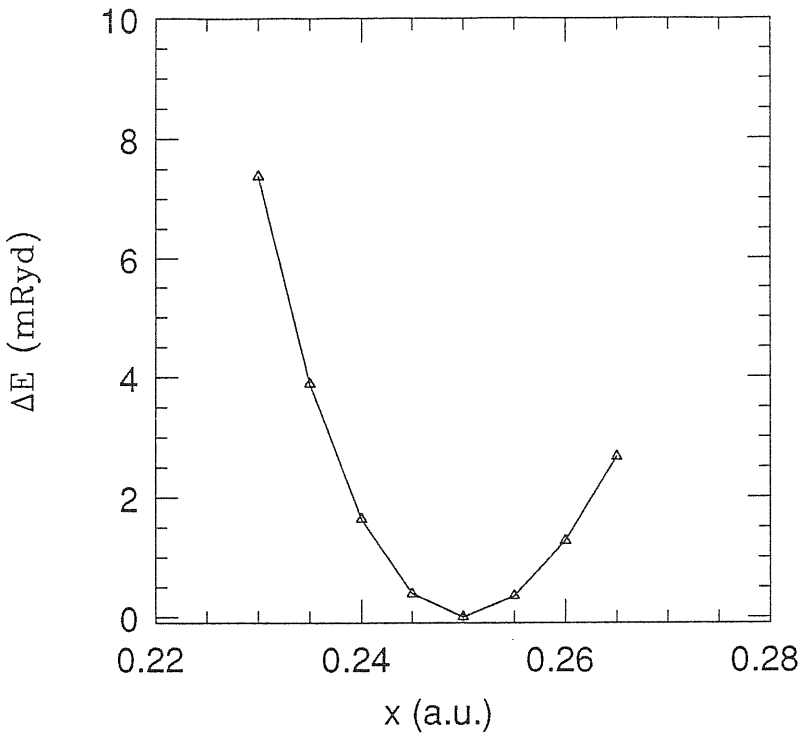

Fig. 7 - Difference in energy as a function of zinc atom position along (111) direction. x=0.25 is the equilibrium zincblende position. Energy unit is mRyd.

The first tellurium forms bonds with one zinc and three cadmium and is an example of the tetrahedron AB_3C, while the second one has three zinc and one cadmium (A_3BC). The lattice constant is set at the value calculated using Vegard law with the pure compounds lattice constants obtained in Sec. II. In Table IV we report the forces appearing in the unrelaxed configuration. What can be immediately seen is that forces acting on tellurium atoms are one order of magnitude larger than those acting on Zn and Cd. This is in agreement with the model used in interpreting EXAFS and X-ray results, where only the tellurium sublattice is allowed to distort. Using the forces we searched for the

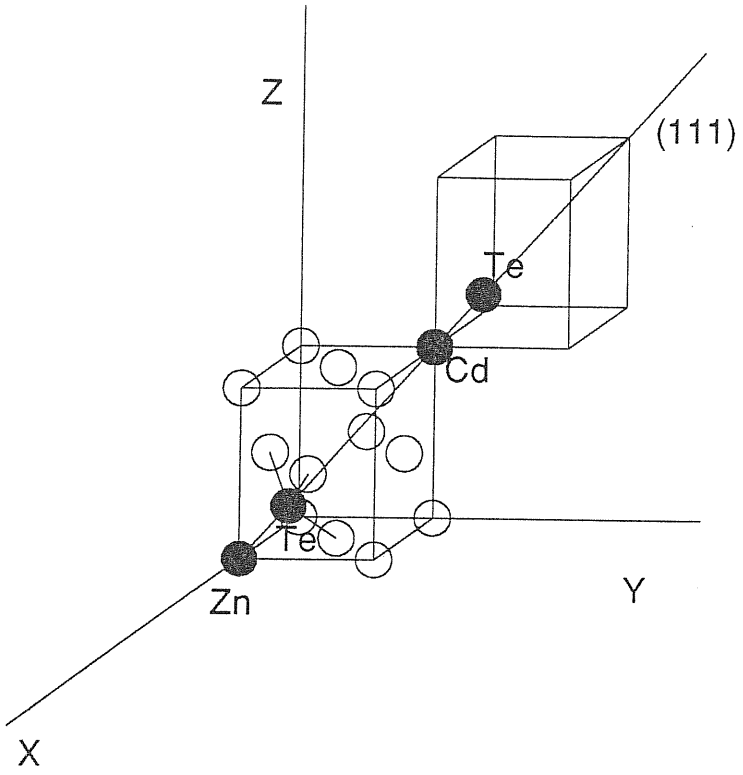

Fig. 8 - (111) supercell used in the calculation. The four black atoms are respectively Zn-Te-Cd and Te and are the basic unit of our system.

relaxed configuration and the result is shown in Table IV where we report the position of the atoms and the forces acting on them. These positions are along the (111) direction, and the measure unit is $a\sqrt{3/2}$

Initial Pos.	F_z(ryd/a.u.)	Final Pos.	F_z
0.0000 (Zn)	1.7×10^{-3}	-0.0003	3.8×10^{-3}
1.4142 (Cd)	-1.7×10^{-3}	1.4146	-2.2×10^{-3}
0.3535 (Te)	-3.1×10^{-2}	0.3403	6.1×10^{-4}
1.7677 (Te)	3.1×10^{-2}	1.7797	-6.0×10^{-4}

Table IV - Initial and final position of atoms in the supercell. The forces are along (111) direction. Distances are measured with respect to the lattice constant (measure unit is a $\sqrt{3/2}$).

The distortion of the two tellurium atoms is different and it is $\Delta_1 = 0.099$ Å, $\Delta_2 = 0.088$ Å in good agreement with X-ray data.

From this simple case we can draw some consideration concerning the ferroelectricity of the alloy. If we calculate the polarization of the relaxed (111) superlattice using a simple ansatz, that is supposing that every atom is an ion with an effective charge equal to the calculated Born effective charge, and assuming that the undistorted lattice has zero polarization we have

$$\vec{P} = \sum_s Z_s(\vec{\tau}_s - \vec{\tau}_{s0}). \tag{17}$$

The result is $P = 0.145 \mu C/cm^2$ in the (111) direction, which is a much higher value than the experimental one. In this case the polarization is due to the different relaxation of the two unequivalent tellurium atoms and to the different effective charges. Clearly our value, calculated for perfect ordering, is an upper

bound for the actual value in a real alloy with $x = 0.5$. The value measured in the alloy depends on composition, on disorder, and on temperature. It is clear that the order of magnitude of relaxation of Te atom is far too large than necessary to give the measured spontaneous polarization, and for this reason in this system ferroelectricity could be related to some unbalance between dipoles pointing toward different directions. The reason of this unbalance can be investigated only including finite-temperature effects and for this reason a statistical mechanics calculation—where all possible tetrahedra are accounted for—is necessary. We have shown that, using *ab-initio* techniques, it is possible to describe realistically the properties of this alloy; this work can be considered as a first step toward a more complete theoretical description.

Acknowledgements

I would like to express my gratitude to my supervisors Raffaele Resta and Stefano Baroni, they introduced me in this stimulating field of electronic structure calculation, proposing me the subject of this work and giving me constant help and continuous encouragement.

A special thank to Stefano De Gironcoli for his numerous explainations of the code used to calculate phonon frequencies and for showing me his results on NLCC.

I am also grateful to Paolo Giannozzi for giving me many routines used to build the pseudopotentials.

I would also like to thank SISSA System Manager, Roberto Innocente for his precious help with the computer system, and finally I want to thank all my friends here in SISSA for the numerous stimulating discussions.

References

[1] R. Weil, R. Nkum, E. Muranevich, L. Benguigui, *Phys. Rev. Lett.* 62, 2744 (1989).

[2] R. K. Nkum, R. Weil, E. Muranevich, L. Benguigui and G. Kimmel, *Material Science and Engineering* **B9**, 217 (1991).

[3] A. Balzarotti, *Physica* **146B**, 150 (1987).

[4] S.-H. Wei, L. G. Ferreira and A. Zunger, *Phys. Rev. B* **41**, 8240 (1990).

[5] G. P. Srivastava, J. L. Martins, A. Zunger, *Phys. Rev. B* **31**, 2561 (1985).

[6] J. L. Martins and A. Zunger, *Phys. Rev. B* **30**, 6217 (1984).

[7] J. E. Bernard and A. Zunger, *Phys. Rev. B* **36**, 3199 (1987).

[8] K. J. Chang, S. Froyen and M. L. Cohen, *Phys. Rev. B* **28**, 4736 (1983).

[9] G. E. Engel and R. J. Needs, *Phys. Rev. B* **41**, 7876 (1990).

[10] A. Qteish, R. J. Needs, *Phys. Rev. B* **43**, 4229 (1991).

[11] S.-H. Wei and A. Zunger, *Phys. Rev. B* **37**, 8958 (1988).

[12] S. G. Louie, S. Froyen and M. L. Cohen, *Phys. Rev. B* **26**, 1738 (1982).

[13] P. Giannozzi, S. De Gironcoli, P. Pavone and S. Baroni, *Phys. Rev. B* **43**, 7231 (1991).

[14] G. B. Bachelet, D. R. Hamann and M. Schlüter, *Phys. Rev. B* **26**, 4199 (1982).

[15] U. von Barth and R. Car, unpublished.

[16] J. Perdew and A. Zunger, *Phys. Rev. B* **23**, 5048 (1981).

[17] F.D. Murnaghan, Proc. Nat. Acad. Sci. USA **50**, 697 (1944).

[18] H. J. Monkhorst and J. D. Pack, *Phys. Rev. B* **13**, 5188 (1976).

[19] H. Hellman, Einführung in die Quantenchemie (Deuticke, Leipzig, 1937); R. P. Feynman, *Phys. Rev.* **56**, 340 (1939).

[20] K. Kunc, in *Electronic Structure, Dynamics and Quantum Structural Properties of Condensed Matter*, edited by J.T. Devreese and P. Van Camp (Plenum, New York, 1985), p. 227.

[21] S. Baroni, P. Giannozzi, and A. Testa, *Phys. Rev. Lett.* **58**, 1861 (1987).

[22] S. De Gironcoli, S. Baroni and R. Resta, *Phys. Rev. Lett.* **62**, 2853 (1989).

[23] K. Kobayashi, Y. Morikawa, K. Terakura and S. Blügel, *Phys. Rev. B* **45**, 3469 (1992).

[24] S. De Gironcoli, *Private Communication.*

[25] W. Kohn and L.J. Sham, *Phys. Rev.***140**,A1133 (1965).

[26] J. M. Rowe, R. M. Nicklow, D. L. Price and K. Zanio, *Phys. Rev. B* **10**, 671 (1974).

[27] P. Plumelle and M. Vandevyver, *Phys. Status Solidi (b)* **73**, 271 (1976).

[28] N. Vagelatos, D. Wehe and J. S. King *J. Chem. Phys.* **60**, 3613 (1974).

[29] S. Perkowitz and R. H. Thorland, *Phys. Rev. B* **9**, 545 (1974).

[30] Q. T. Islam and B. A. Bunker, *Phys. Rev. Lett.* **59**, 2701 (1987).

[31] J. C. Mikkelsen and J. B. Boyce, *Phys. Rev. Lett.* **49**, 1412 (1982).

[32] S.-H. Wei and A. Zunger, *Phys. Rev. B* **43**, 1662 (1991).